

# Chapter 8

## Rainfall Prediction for Landfalling Tropical Cyclones: Perspectives of Mitigation

Kevin K. W. Cheung, Lisa T.-C. Chang and Yubin Li

**Abstract** The torrential rainfall associated with landfalling tropical cyclones (TCs) often represents the major impact to coastal regions, but at the same time an enormous challenge to meteorologists and forecasts. This chapter first discusses the complex dynamical processes involved in TC landfalls, which are related to the increased surface roughness and reduced surface moisture fluxes of land. The result is often certain patterns of convection and rainfall asymmetry in the landfalling TCs, but these patterns are not well explained by current theories or conceptual models. With emphasis of development of rainfall prediction techniques according to the needs of mitigation, the requirements on the skill of rainfall forecasts from the perspectives of mitigation are reviewed. Then, the operation and performance of several statistical TC rainfall models are discussed including the rainfall climatology-persistence model (R-CLIPER) for the Taiwan area. A topographic component is developed for R-CLIPER through multiple regression analyses, which improves the model's performance in reproducing the local extreme rain that is lacking in the original model. Finally, the importance of utilizing remote-sensing data in TC rainfall prediction is discussed, and how TC rainfall statistical models can be applied to risk analyses under the consideration of global changes.

---

K. K. W. Cheung (✉) · Y. Li  
Department of Environment and Geography, Macquarie University,  
Sydney, NSW 2109, Australia  
e-mail: kevin.cheung@mq.edu.au

L. T.-C. Chang  
Department of Environmental Management, Tunghan University, New Taipei City, Taiwan

L. T.-C. Chang  
Risk Frontiers Natural Hazards Research Centre, Macquarie University, Macquarie,  
Australia

Y. Li  
School of Energy and Environment, City University of Hong Kong, Kowloon, Hong Kong

**Keywords** Tropical cyclone rainfall · Landfall processes · Climatology-persistence model · Topographic effect · Orographic rain · Mitigation

*Prepared for “Remote Sensing of Typhoon Impact and Crisis Management”.*

May 2011

## 8.1 Introduction

Tropical cyclones (TCs) are severe weather systems that develop over most of the ocean basins, and thus their impacts are worldwide that include the Gulf and East coast of the U.S., South East Asia, India, the tropical Australian regions as well as African countries located by the Southwest Indian Ocean. It is well known that the hazards associated with TCs are multiple in nature and mutually interconnected. Direct damages to infrastructure may mostly due to the destructive winds within the core circulation of TCs, however, very often it is the torrential rainfall accompanying most TCs that bring huge economic loss and even that of human lives. Moreover, the coastal areas are exposed to the risk of storm surges that could be disastrous and may have more extensive areas of impact than the TC landfall location. Given this wide range of sources of hazards, however, their relative impacts in various geographic locations highly vary. This is partially due to the fact that there are different characteristics of TCs that developed in different ocean basins. For example, it is known that TCs in the western North Pacific have a larger average size compared with those in other ocean basins, and thus possibly have a larger radius of gale-force winds when the extent of impact is considered. On the other hand, the local geography, persistent synoptic situations and topography often determine the nature of hazards that would occur in a particular region.

Since there is no weather station and rain gauge to measure rainfall over the oceans, estimation of rainfall from TCs before they make landfall relies on satellite observations, which are only available in the recent few decades. Different algorithms for estimating rainfall exist depending on which part of the electromagnetic spectrum that the satellite observations are from. For example, there are algorithms that estimate rain rate from just the brightness temperature of the infrared-channel satellite imageries (Ebert et al. 2007). Due to the capability of penetrating into clouds and that microwave emission and scattering are more directly related to precipitation, passive microwave data is considered superior compared with IR algorithms in rain rate estimation. An example is the satellite that was launched in the Tropical Rainfall Measuring Mission (TRMM) by the National Aeronautics and Space Administration (NASA) in 1997, which included the TRMM Microwave Imager (TMI). Moreover, the TRMM satellite platform was the first to have the precipitation radar installed, which was often taken as the reference for

calibrating IR and microwave algorithms. Based on TMI rain rate estimates, Lonfat et al. (2004) examined the rainfall distribution within TCs over the global oceans. It was found that for azimuthally averaged rain rate, the radial profile (or variation) is similar to that of wind speed with a maximum near the eyewall. The maximum rain rate of about  $12 \text{ mm h}^{-1}$  was found for the most intense TC category of Cat 3-5 according to the Saffir-Simpson hurricane scale (Simpson 1971; Saffir 1977). When TCs intensify, the average radius with maximum rain rate decreases from about 50 km for tropical storms (systems with sustained near-surface wind speeds larger than 34 kt or  $17.5 \text{ m s}^{-1}$ ) to about 35 km for Cat 3-5 TCs. On the other hand, the asymmetric component of rainfall distribution in TCs was found to concentrate at the front quadrants with respect to the motion vector, which is related to convergence between the TC circulation and the environmental flow (Fig. 8.1). For tropical storms in the Northern Hemisphere, the maximum rain

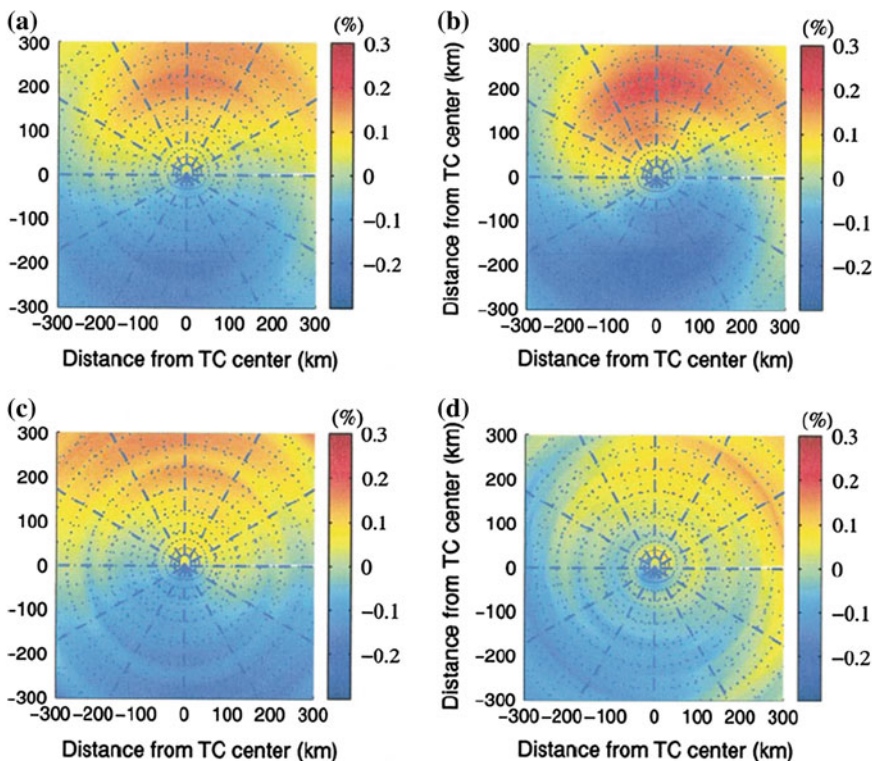


**Fig. 8.1** Rainfall asymmetry calculated in 10 km rings around the storm center, as a function of storm intensity: **a** 2121 TC observations from TCs globally, **b** TS, **c** CAT12, **d** CAT35. The storm motion vector is aligned with the positive y axis. The color scale indicates the amplitude of the normalized asymmetry. The *red* corresponds to the maximum positive anomaly and the *blue* the minimum rainfall within the storm [adapted from Lonfat et al. (2004)]

rate is likely in the front-left quadrant, and then shifts to the front-right quadrant when intensify to the Cat 3-5 more intense TCs.

When TCs make landfall, rain gauges installed over land provide a valuable source of in situ observations of rain rate within the TCs. However, rain-gauge networks usually do not have enough spatial resolution to resolve the detailed rainfall distributions within TCs and identify extreme rain rates. For these purposes, land-based Doppler radar systems serve much better to monitor torrential rainfall because the spatial resolution of the reflectivity data from most radar systems is of the order of kilometers, and rain estimates based on radar reflectivity can have resolution about 2–3 km or even better (e.g., Chen et al. 2007). Although there are issues such as topographic effect to radar-based rain estimation, a lot of algorithms have been developed to suit rainfall systems with different origins such as those from the tropics and midlatitudes (e.g., Krajewski et al. 2010). Advanced radar techniques such as measurement of the raindrop size distributions in clouds largely increase the capability of more accurate rain estimate based on radar data. Moreover, there are mobile radar systems that have been developed to observe the local-scale convective systems especially those in mountainous regions where blocking and orographic lifting effect may reduce the quality of the data from fixed-platform radar systems. That is to say, there is wealth of land-based observations to monitor the structural changes associated with landfalling TCs including their convection and rainfall distributions.

Since TCs are weather systems with extreme wind speeds within, when they make landfall the sudden change in the surface roughness imposes modifications in the boundary-layer winds. In general, the near-surface winds over land will be reduced in speed that represents low-level convergence, and this may lead to enhanced convection and rainfall that subsequently extend the effect of landfall up to higher levels. However, land surfaces usually have less moisture fluxes compared with those over ocean, and the effects to convection may not be simple. Nevertheless, this kind of structural changes associated with surface roughness and moisture fluxes always interact with the TC circulation itself as well as the ambient environment, which result in a series of complex dynamical feedback processes during landfall. Some of the previous researches developed conceptual models of TC landfall based on idealized modeling, but few results from these simulations have actually been verified by observations. Thus, more conclusive explanations of the structural changes associated with TC landfalls have yet to be identified, and the state of the science is reviewed in Sect. 8.2. For risk analysis and mitigation purposes, more efficient rainfall estimation methodologies are often needed such that a large number of different hazard scenarios can be analyzed. Given that to at least the first order the rainfall distributions in TCs can be described by certain statistical distributions, it is feasible to estimate the rainfall scenarios of landfalling TCs based on some kinds of statistical models that take information from TC track forecasts, rainfall climatology and other possible effects such as topography. Some recent research in this aspect is discussed in Sects. 8.3 and 8.4. After that, Sect. 8.5 briefly discusses the potential impacts to trends of TC rainfall from natural and anthropogenic global changes, and a summary is given in Sect. 8.6.

## 8.2 Dynamical Processes that Govern the Structure and Rainfall Distribution of Tropical Cyclones During Landfall

### 8.2.1 Dissipation Over Land

The intensity of a TC is defined as either the maximum surface wind or the minimum central surface pressure (Wang and Wu 2004). Specifically, maximum surface wind is directly associated with damages and impacts caused by TCs, and when it is used to represent the intensity the wind speed at height of 10 m averaged over a period of 1 min (for U.S. agencies) or 10 min (most of the other regions) is referred to. When TCs develop over the oceans, influences on intensity include inner-core characteristic, large-scale atmospheric flow especially the vertical wind shear, ocean processes and interactions between air and sea (e.g., Kaplan et al. 2010). When TCs make landfall, ample observational and theoretical evidence show that TCs decay rapidly and finally dissipate as they move over land, because they are primarily maintained by the latent heat release of water vapor extracted from the oceans (Wong et al. 2008 and references therein). However, a lot of factors affect how the intensities of TCs vary before and after landfall. For TCs that made landfall at the U.S. Gulf coast, statistical results show that on average the weakest TCs strengthen at most before landfall, and the strongest hurricanes weaken the most, with the threshold of intensity separating the two groups about 85–100 kt (1 kt =  $0.514 \text{ m s}^{-1}$ ; Rappaport et al. 2010). Previous studies show that the decay rate of TCs is related to their respective central pressures at landfall, and the wind speed decays to a small but nonzero background wind speed (Schwerdt et al. 1979; Ho et al. 1987; Kaplan and DeMaria 1995; Wong et al. 2008; Ramsay and Leslie 2008). Based on the data of U.S. landfalling TCs during the period 1967–1993, Kaplan and DeMaria (1995) developed an empirical model for predicting the maximum wind of landfalling TCs. In the model, the wind speed is determined from a simple two-parameter exponential decay function. An optional correction can also be added that considers storms that move inland slowly or rapidly. This model from Kaplan and DeMaria can explain 91 % (93 % if the motion speed correction is made) of the variance in intensity change after landfall. On the other hand, Wong et al. (2008) developed a similar model for South China coast landfalling TCs based on a dataset during 1975–2005. Besides the landfall intensity and landward speed, it was found that excess of 850 hPa moist static energy has significant influence on the intensity decay rates.

### 8.2.2 Complex Interactions of the Dynamical Processes

The structure of a TC is characterized by its wind, pressure, temperature fields and water distribution. Many factors determine TC structure such as the size of the low-level cyclonic circulation as measured by the outermost closed isobar or the

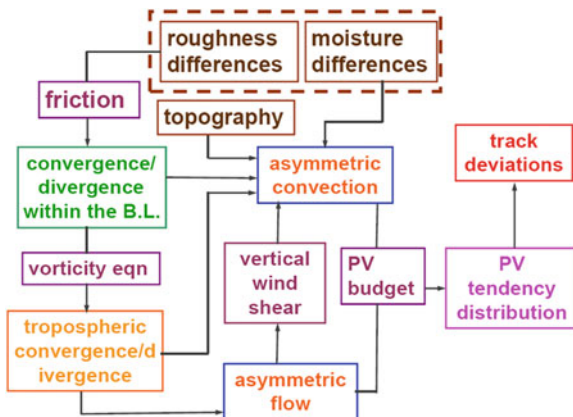
radius of sustained gale-force winds, the radius of maximum wind (RMW), the convection distribution including that at the eyewall, and both the inner and outer spiral rainbands (Chan et al. 2004; Dastoor and Krishnamurti 1991; Wang and Wu 2004). Numerous studies have been conducted to understand how land surface affects the structure of TCs (Chang 1982; Bender et al. 1985, 1987; Dastoor and Krishnamurti 1991; Chang et al. 1993; Zehnder 1993; Yeh and Elsberry 1993a, b; Lin et al. 1999; Wu and Kuo 1999; Wu 2001; Farfan and Zehnder 2001; Wu et al. 2002, 2009; Ramsay and Leslie 2008). The results from these studies generally show that when a TC is getting close to the coast, the outer circulation of a TC interacts with the land region and have significant influence on the TC's structure. Firstly, the surface wind speed over land is significantly reduced owing to the increased surface roughness, while the turbulent kinetic energy over land is obviously enhanced for the same reason (e.g., Ramsay and Leslie 2008). Secondly, the moisture supply is different between the on-shore and off-shore winds (e.g., Tuleya and Kurihara 1978). Besides, the moisture supply is also affected by mesoscale systems introduced by land-sea difference and influences from monsoon (e.g., Gao et al. 2009). Thirdly, topography near the coastal region imposes additional mechanisms that affect TC structure during landfall. The orographic lifting effect highly enhances rainfall at the windward side by forcing convection, but the resulted rainfall distribution is sensitive to the location of landfall and movement speed of the TC (Lin et al. 2002; Wu et al. 2002). On the leeward side, down-slope winds can be generated, and large turbulent eddies enhanced by complex terrains may transport strong winds to the surface (e.g., Ramsay and Leslie 2008).

These effects are organically connected together, and will further affect the TC structure by interacting with each other and with the ambient environment, which makes the processes associated with structure changes of landfalling TCs even more complicated (Chan 2010; Fig. 8.2). For example, the changed surface wind and moisture field over land will further affect the upper-level atmosphere through momentum and moisture exchange. The consequent may be changes in the vertical wind shear, which is another critical factor to determine the development of convection within the TC. Through the tangential and vertical winds of TC circulation, the aforementioned effects can be advected back to the offshore areas over the sea and/or upper levels, which leads to the question of whether there are guidelines in estimating the asymmetry of rainfall during TC landfall?

### ***8.2.3 Asymmetry in Convection***

Accurately forecasting the precipitation pattern of landfalling TCs is of significant value, as the torrential rainfall accompanying a TC cause major threats to the coastal areas. The TC rainfall distribution is determined by many factors, including, but not limited to, environmental factors such as vertical wind shear, sea surface temperature, moisture distribution, as well as the TC-specific factors such as

**Fig. 8.2** Schematics to show the feedback processes between the land-sea roughness difference, moisture difference, topography, asymmetric flow and convection, and the resulted TC track deviations [adapted from Chan (2010)]



intensity, location, and translation speed (Lonfat et al. 2004). The average axisymmetric distribution of rainfall within a TC is an intense-rainfall ring that is associated with the eyewall convection and the rainbands that extend from the storm center. However, in reality TC rainfall distributions may have large deviations from this average distribution, which sometimes are caused by environmental factors (e.g., monsoonal effects) or mesoscale systems embedded within TCs.

When a TC is approaching land, the friction-induced convergence in the boundary layer will affect its precipitation pattern (e.g., Marks 1985). Early studies such as Koteswaram and Gaspar (1956), Dunn and Miller (1960), and Miller (1964) already observed this asymmetry in rainfall pattern and explained that this frictional convergence is induced to the right side of a landfalling TC, which follows the on-shore flow, in the Northern Hemisphere and strengthen the rainfall there. Later observational and numerical studies also claimed that coastal rainfall inclines to the right of the track of Northern Hemisphere TCs (Tuleya and Kurihara 1978; Jones 1987; Powell 1987). However, other studies have also found convective activity to be more pronounced to the left of the track (e.g., Parrish et al. 1982; Blackwell 2000; Chan and Liang 2003; Chan et al. 2004). Examination of several TC landfall cases over the South China Sea in Chan et al. (2004) showed that enhanced convection occurs to the west of the TC (i.e., to the left of track) in the mid- to lower troposphere and was then advected to the southward side (i.e., off shore) of the upper troposphere by cyclonic flow and rising motion. For this type of disagreement on the location of enhanced rainfall, Powell (1982) explained that the frictional convergence reasoning cannot be the only determining factor of the coastal rainfall maximum, but other parameters such as local topography can also be in action. The idealized simulations in Chan and Liang (2003) further this point in that even without topography, the less moisture fluxes from land can possibly increase the convective instability and enhance rainfall. Then the area of enhanced convection is advected by the TC circulation to regions that are different from the on-shore location where the strongest frictional convergence is found. Meanwhile in the Southern Hemisphere, observational studies show that the rainfall is stronger

in the left side of TC track that is consistent with the location of enhanced frictional convergence (Lonfat et al. 2004). Ramsay and Leslie's (2008) numerical study made it clear that when the topography effect was removed, the rainfall was obviously moved to the left side when TC Larry (2006) was landfalling, while with the topography effect the opposite result appeared, which is in agreement with Powell's (1982) explanation. However, Li et al. (2011; 2013) recently examined several TC landfall cases at northwestern Australia where topography effect is minimal (Fig. 8.3). It was found that low-level frictional convergence cannot fully explain the observed asymmetry in convection, while physical processes as in the aforementioned idealized simulation including feedbacks to the ambient environment may play important roles.

### 8.3 Statistical Models to Estimate Tropical Cyclone Rainfall During Landfall

#### 8.3.1 Consideration of Requirements from Mitigation

There have been substantial improvements in the skill of numerical weather prediction (NWP) models for simulating rainfall in the recent decade, which partially attribute to fundamental improvements in the physical process representations in

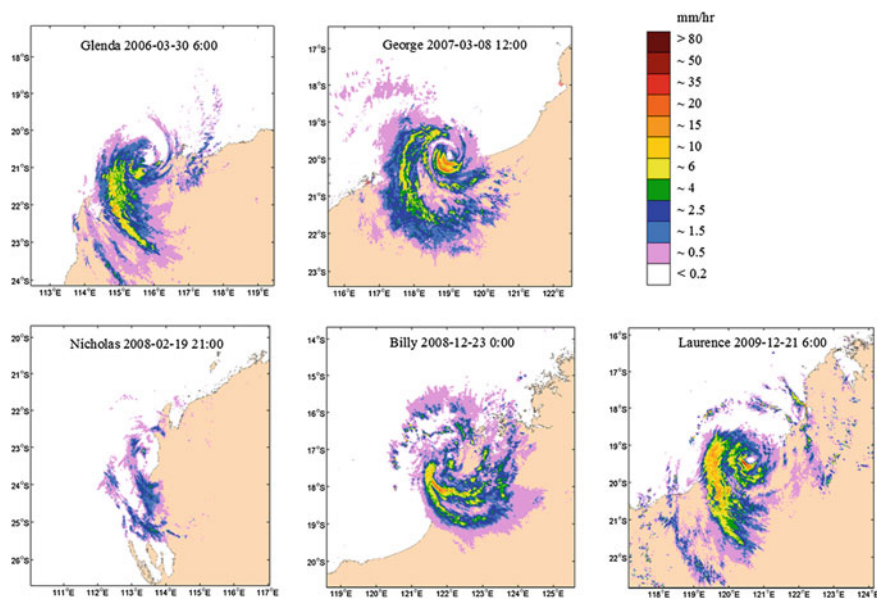


**Fig. 8.3** Rain rate estimates from radar reflectivity prepared by the Bureau of Meteorology for five landfalling TCs at northwestern Australia showing their asymmetry in convection distributions [adapted from Li et al. (2011, 2013)]



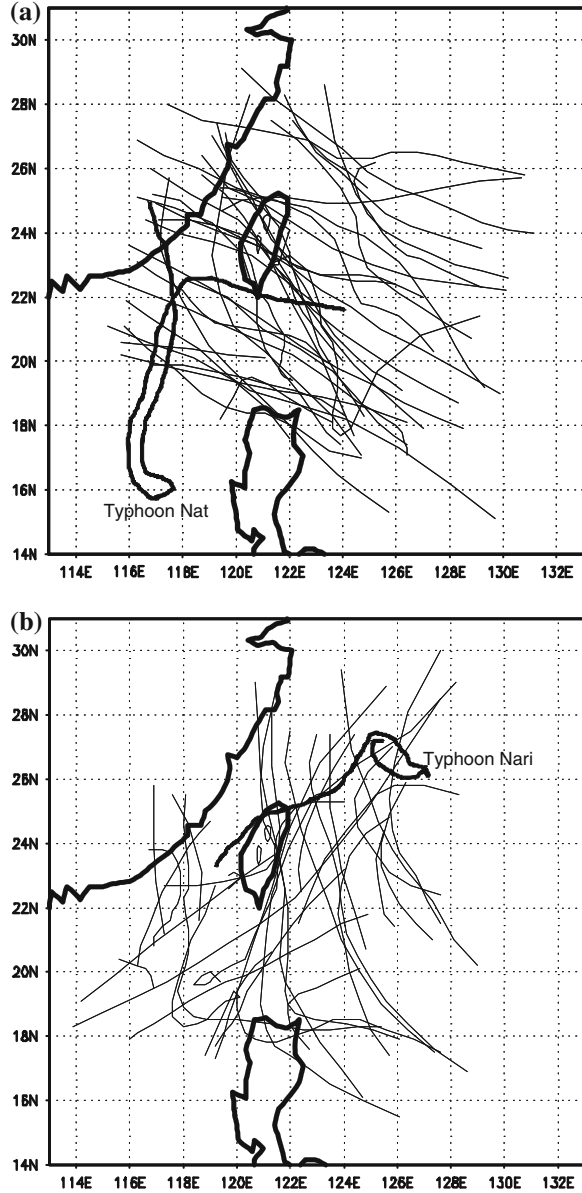
the numerical models. In addition, the availability of high-performance computing resources allows explicit simulations of the rainfall systems such as TCs rather than relying on the so-called cumulus parameterization schemes that are sources of large uncertainties in rainfall simulations. Explicit moisture or cloud-resolving simulation is a trend of development in global general circulation models as well.

Given these advances in NWP models, their applications in rainfall forecasts for mitigation purposes do not always benefit because sometimes the models' performances vary largely with the timescales concerned. The multiple nature of hazards associated with TCs, however, need accurate rainfall forecasts within a wide range of timescales. For example, flash flood potential estimation requires that the extreme rain rate within hours be well captured (e.g., Chen et al. 2008). For estimation of the extent of flood events, good estimates of the accumulated rainfall over a longer period of time are necessary. Similarly for landslide and debris flow potential estimation because the avalanche processes depend much on the absorbed water in the slopes within days, and thus the accumulated rainfall at particular locations is of most concern. However, very often NWP models are tuned to perform best at a specific timescale only, through either settings in the physical process representations or post processing. This is the reason why different techniques of rainfall estimation other than NWP models are utilized in mitigation. For nowcasting, rainfall estimation algorithms based on radar reflectivity data are widely applied (e.g., Chen et al. 2007). For accumulated rainfall estimation from timescales of hours to days, statistical models of rainfall are common practices because they have the additional advantage of able to generate a large number of different rainfall scenarios with much shorter time compared with running an ensemble of dynamical models. These statistical rainfall models, which are usually developed for specific weather systems, have the limitations of low ability to reproduce extreme rainfall events and that they are not simulating the realistic environment such as topographic effect. The following sections describe several TC-related statistical rainfall models and their recent developments.

### ***8.3.2 The Rainfall Climatology-Persistence Model for the Taiwan Area***

Cheung et al. (2008) examined the TC rainfall characteristics in Taiwan and evaluated the The rainfall climatology-persistence (R-CLIPER) model. The following discussions are based on the Cheung et al. study. The spatial characteristics of TC rainfall is studied by first setting up climatology based on the 62 TC cases that passed through the domain 118°–126°E, 18°–27°N during 1989–2002 (Fig. 8.4). When one of the 62 TC tracks passes through one of the grids in the domain, the rainfall data of the 371 rain gauges in Taiwan are recorded. Thus after examining all 62 TC cases, statistics on the average, maximum and minimum rainfall, standard deviation and the number of TCs ever passed through each grid

**Fig. 8.4** The (a) 34 East–West-oriented and (b) 27 south–north oriented TC tracks during 1989–2002 in the Taiwan area. Note the special track types of Typhoons Nat (1991) and Nari (2001) [adapted from Cheung et al. (2008)]



box and for each rain gauge are obtained. In other words, for each rain gauge there is a map of rainfall describing the climatology of that particular station when a TC is situated at different position in the domain (Fig. 8.5). For example, Fig. 8.5 indicates that Taipei station (46692) will be receiving more rainfall when the TC center is located northeast of Taiwan or over land west of the Central Mountain Range (CMR; Fig. 8.6).

**Fig. 8.5** Computation domain and the  $0.5^\circ \times 0.5^\circ$  latitude/longitude grid boxes used in computing the statistics of TC rainfall during 1989–2002. The rainfall climatology map shown is for the Taipei station (46692) after a Barnes objective analysis to a fine  $0.1^\circ \times 0.1^\circ$  latitude/longitude grid [adapted from Cheung et al. (2008)]

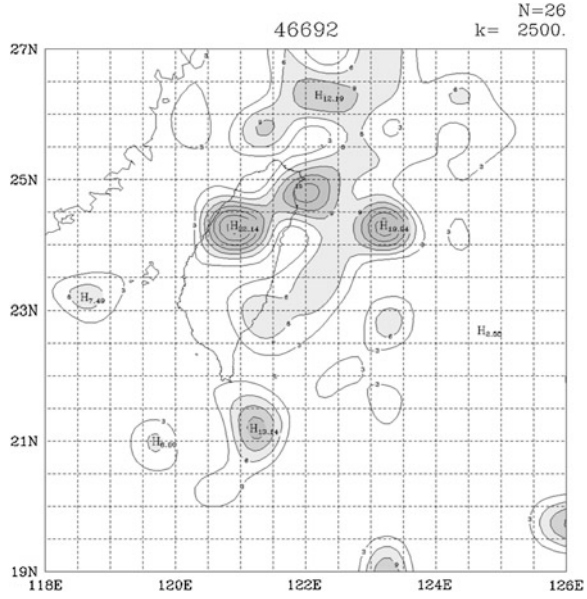


**Fig. 8.6** Topography of Taiwan showing the Central Mountain Range with contour levels of 500, 1,500 and 3,000 m [adapted from Chang et al. (2011)]



The R-CLIPER model is a simple weighted combination of TC rainfall climatology and persistence for estimating rainfall in the future (Lee et al. 2006). Whenever an official forecast track from the Central Weather Bureau is issued, it is first spatially interpolated such that hourly positions are available. Then the climatological rainfall map for each of the 365 main-island stations is looked up in turn to obtain the climatology value for a particular TC center position. When this rain amount is accumulated along the forecast TC track, the rain distribution within a certain forecast period (i.e., the climatology component of R-CLIPER) is obtained. Next the persistence component of R-CLIPER is determined. Various tests based on maximizing the pattern correlation between R-CLIPER forecast rain and observed value on the persistence duration indicate that a 3-h period, which is typical convective timescale, is optimal to project a reasonable short-range rainfall estimate. For determining the relative contributions from climatology and persistence in the final rainfall prediction, optimal pattern correlation is realized when the ratio of climatology to persistence is 4/6 (7/3) in the 0–3-h (3–6-h) time period, and then only climatology is used after 6 h.

Verification of R-CLIPER based on independent TC cases finds that the root-mean-square error ranges from 11.4 mm for 3-h accumulated rain to 86.6 mm for 24-h accumulated rain, indicating that the R-CLIPER does provide reasonable estimates of rainfall amount in the short range. Equitable threat score (ETS), which measures the number of forecasts (locations) that match the observed threshold amount (Tuleya et al. 2007; see definition in Cheung et al. 2008) is used to further evaluate the rain prediction skill. For 24-h forecasts, the ETS values of 0.22, 0.13, 0.08 and 0.04 are obtained for the thresholds of 50, 130, 200 and 350 mm, respectively. These ETS values are similar to those of the R-CLIPER for Atlantic hurricane rainfall (Marchok et al. 2007). In Cheung et al. (2008) more verification are performed with ETS values for shorter forecast periods and for individual stations such that the geographic distributions of the model's performance can be examined. Several TC cases are also used to illustrate the applications of R-CLIPER. The readers are referred to that chapter for details.

### ***8.3.3 Recent Developments***

Since the R-CLIPER uses the rainfall climatology (average of historical TC cases in the model database) as the major component in the model, it often underestimates the observed rainfall especially for the extreme rainfall in mountainous regions (Cheung et al. 2008). Lee et al. (2008) improved the original R-CLIPER and developed a version 2.0 of the model. The major aspects of improvement are stratifications of the rainfall estimation according to river basins, TC track types, intensity and size. For example, rainfall climatology usually accounts for only about 30–40 % of the observed value, but this percentage varies for different river

basins. Thus, it is found that for some river basins the rainfall estimation can be improved by calculating the average of the higher rainfall in the historical database and replacing the climatology component in the model, which is referred to as ‘threshold adjustment’ in Lee et al. (2008).

The above-mentioned adjustment procedure is certainly case dependent. Through examination of many typical TC cases in the Taiwan area, Lee et al. (2008) found that for the westward-moving TCs that make landfall to Taiwan, correlation between rainfall and intensity is higher than other parameters because the severe convection in the intense TCs is bringing direct impact to the landfall location together with torrential rainfall. On the other hand, for the TC tracks that pass through the Taiwan area but are quite distant from the island, the correlation between rainfall and TC size is higher because the more extensive rain bands usually accompanying the larger TCs have better chance of bringing heavy rainfall to the island even though TC centers do not make landfall at all.

The essential philosophy of the R-CLIPER version 2.0 is its flexibility to adjust the climatology component in different river basins, i.e., what percentile of the historical extreme rainfall to retain. The adjustment procedure is a semi-subjective process of identifying some historical analogues (usually TC cases with similar tracks) of the real-time forecast case, and then assigning appropriate ‘thresholds’ to the river basins according to the intensity and size of the current TC under forecast.

By way of example from Lee et al. is the case of Typhoon Krosa (2007) that moved westward and then northwestward and made landfall at northeastern Taiwan (Fig. 8.7). The original R-CLIPER estimates heavy rainfall only at the landfall location and near the core of the Typhoon, but actually the heaviest rainfall occurred in central to southwestern Taiwan. By adjusting the climatology component in individual river basins according to some historical analogues and the fact that Typhoon Krosa had a quite large radius of gale-force winds ( $\sim 300$  km), the estimation of accumulated rainfall distribution from the new R-CLIPER is much improved over the original version.

## 8.4 Topographic Effect

The Taiwan R-CLIPER discussed in the last section does not consider topographic effect explicitly, although the effect was embedded in the rainfall climatology. Similar situation applies to the Atlantic version of R-CLIPER that utilizes rain estimates from the TMI and derives storm-centered mean rain rate distribution stratified for different TC intensities (Marks et al. 2002). This mean rain rate distribution is azimuthally symmetrical, and when accumulated rain amount is computed along the forecast TC track, the rainfall distribution is also symmetrical with respect to the track, which is not realistic. This is why Lonfat et al. (2007)

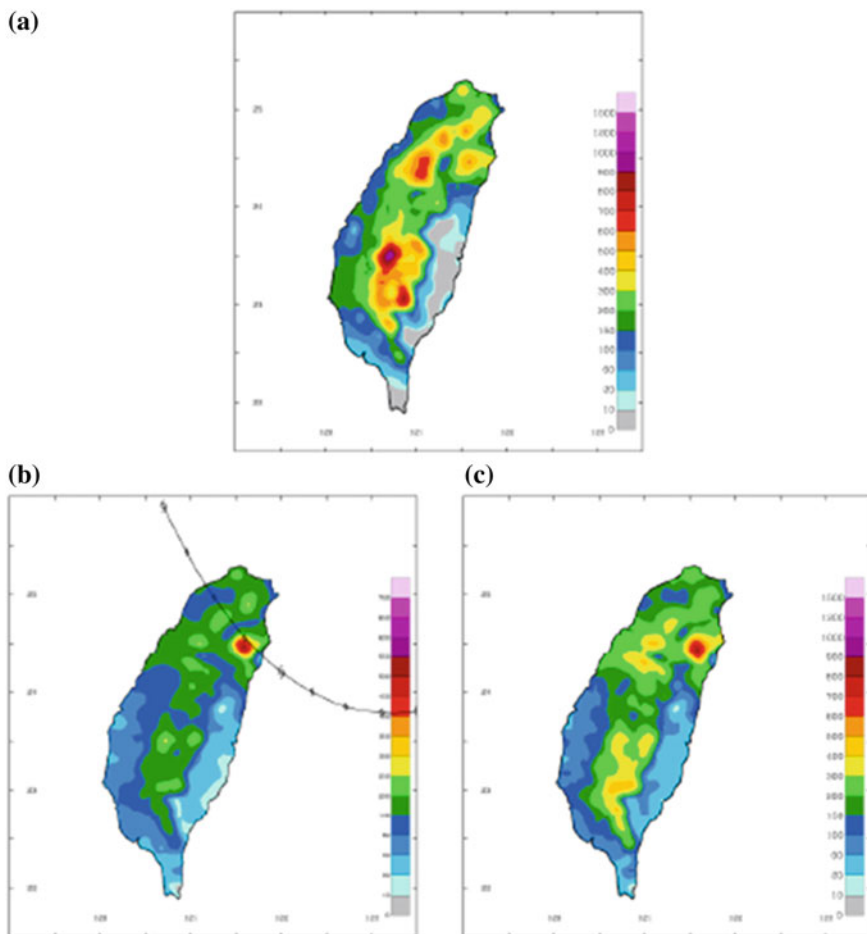


**Fig. 8.7** a Observed, b estimate from the original R-CLIPER, and c estimate from the R-CLIPER version 2.0 of accumulated rainfall distribution for Typhoon Krosa (2007) during the period when the Typhoon was in the model domain [adapted from Lee et al. (2008)]

developed the Parametric Hurricane Rainfall Model (PHRaM) that adds a vertical wind shear term and a topography term to the original R-CLIPER model equation. The effect of topography is modeled by evaluating changes in elevation of flow parcels within the storm circulation and correcting the rainfall field in proportion to those changes (Fig. 8.8). Chang et al. (2011) carried out similar effort to make the Taiwan version of R-CLIPER considers topographic effect explicitly in order to improve the model's ability to estimate extreme rainfall. The following discussions are based on the Chang et al. study.

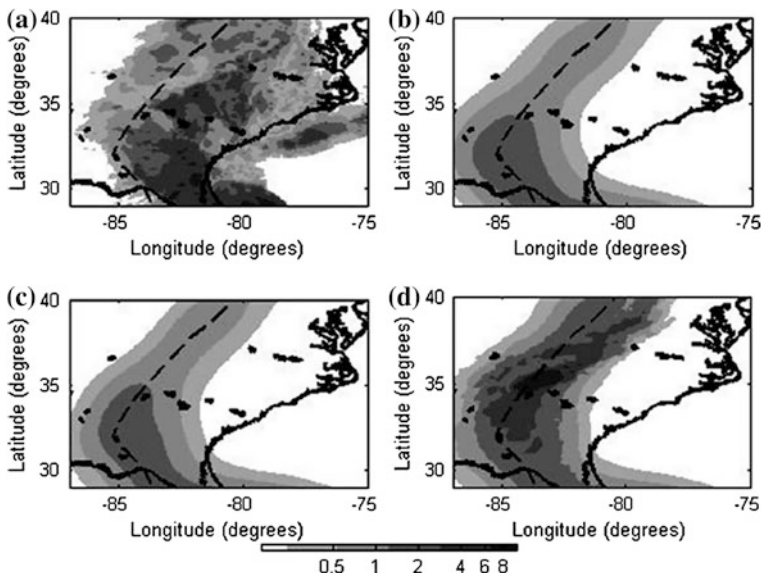


**Fig. 8.8** Rainfall accumulation (in.) in Hurricane Frances (2004) for its second U.S. landfall: **a** stage-IV observations, **b** R-CLIPER, **c** PHRaM-NoTopo, and **d** PHRaM. The *dashed line* indicates the best track for Frances [adapted from Lonfat et al. (2007)]

### 8.4.1 Correlation Between Orographic and Observed Rainfall

The 33 river basins of Taiwan are divided into 5 groups (Fig. 8.9): three to the West (named W1 to W3) and two to the East (E1 and E2). The advantage of analyzing according to the river basins is that if there is heavy rainfall at the catchment area, subsequent flood likely occurs at the lower-level plain area. Thus, additional statistical analyses are also performed for rain stations with high altitudes (>200 m) in order to isolate the effect from topography to the large slopes at the CMR.

The individual relationships between observed rainfall, climatology and orographic rain are examined. For this purpose, linear regression equation in the form of  $y = ax + b$ , where  $x$  and  $y$  are the variates, are fitted to observed 24-h accumulated rainfall from the rain stations in Taiwan and either the climatology values or orographic rain estimates. The same flux model as in the preliminary investigation in Cheung and McAneney (2008) is used to calculate the orographic rain. The model considers orographic lifting of horizontal winds and assumes that all lifted moisture is transformed to rainfall (Lin et al. 2002; Chang et al. 2008). Namely,

$$ORO = (d_a/d_w) \times E \times (\mathbf{V} \cdot \nabla H) \times q \times (L_s/C_s)$$

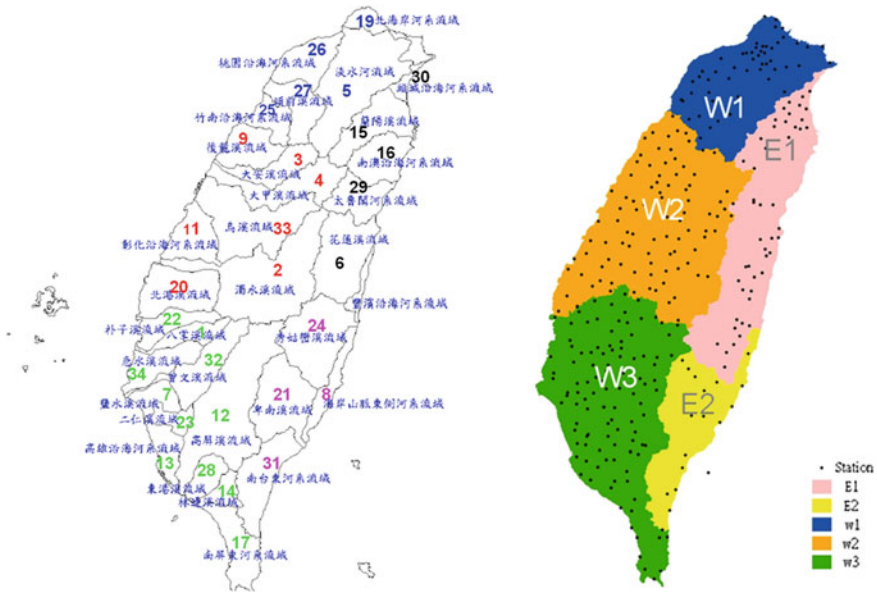


**Fig. 8.9** The 33 river basins in Taiwan (*left panel*), which are separated into five groups E1–E2, W1–W3 with locations of the rain stations (*right panel*) [adapted from Chang et al. (2011)]

where  $d_a$  and  $d_w$  are the density of air and water respectively,  $E$  rainfall efficiency assumed to be 1.0,  $\mathbf{V}$  horizontal wind vector,  $\nabla H$  terrain gradient, and  $q$  the mixing ratio or specific humidity.  $(L_s/C_s)$  measures the length scale and speed of a mesoscale convective system that passes through a point of interest and has the unit of time, and is assigned 24 h for our estimation of accumulated rainfall.

When the explained variances ( $R^2$ ) in the linear regression are examined, it is found that climatology explains from nearly 50 % to about 66 % of observed rainfall (Table 8.1), which are consistent with the results from similar analyses for

**Table 8.1** Explained variance  $R^2$  of observed rainfall by climatology and orographic rain estimate, respectively for all stations or only those with altitude above 200 m

	$R^2$ (Obs-Clim) all stations	$R^2$ (Obs-Clim) stations >200 m	$R^2$ (Obs-Oro) all stations	$R^2$ (Obs-Oro) stations >200 m
W1	0.486	0.412	0.166	0.193
W2	0.562	0.507	0.115	0.191
W3	0.573	0.569	0.103	0.148
W123	0.542	0.502	0.110	0.148
E1	0.597	0.611	0.119	0.186
E2	0.662	0.633	0.174	0.264
E12	0.604	0.620	0.140	0.229

W123 represents the combined western regions, and E12 the combined Eastern regions of Taiwan



R-CLIPER in Cheung et al. (2008). The  $R^2$  values for the Eastern regions are all higher than those for the western region, which indicates that more complex processes are affecting rainfall in western Taiwan, such as TC structures changed by the CMR and monsoon effects. Thus, rainfall estimation based on simple climatology or R-CLIPER is more reliable at Eastern Taiwan than in the western region. As expected, the orographic rain estimate explains less percentage of the observed rainfall, which ranges from 10 to 20 %. The increasing trend in  $R^2$  from West to East is not clear because it is a single mechanism of topographic effect under consideration in this calculation, and the East–West contrast is not the dominating factor.

The explained variances for rain stations with altitude higher than 200 m are also examined. For these rain stations on the slopes, the  $R^2$  values between observed rain and climatology change only little compared with all stations. The slight decreases in  $R^2$  likely attribute to smaller number of stations in calculating the statistics. However, it can be seen that orographic rain can explain more variance of observed rainfall for those rain stations on the mountains with an increase from a few percents to nearly 10 %. Thus, the mechanism of orographic lifting does contribute more to the total rainfall at the slopes compared with plain areas, which has implications for further TC rainfall model development especially with respect to the consideration of regional dependence.

### 8.4.2 Multiple Regression Analyses

In order to explicitly take into account the contribution from topographic effect in TC rainfall estimation, a multiple regression model is established for 24-h accumulated rainfall. The model takes the form

$$\text{OBS} = A1 \times \text{ORO} + A2 \times \text{CLIM} + B,$$

where OBS, ORO and CLIM are observed accumulated rainfall, orographic rain as calculated with the above formula, and the climatology value, respectively.  $A1$ ,  $A2$  and  $B$  are the regression coefficients. The regression is performed for all the 62 TC cases as in R-CLIPER, for each of the regions (W1–W3, E1–E2) as well as the combined regions of W123 (i.e., all western stations) and E12 (i.e., all Eastern stations). There are a total of 37,752 pieces of data that includes all TC cases and stations over Taiwan, and then these data are partitioned into different regions. Due to the different number of TCs that passed through each of the sub-regions, the available number of data that is put into the regression varies from region to region. For example, the western regions of W123 has 20,416 pieces of data and the Eastern regions E12 has 3,504 (columns termed No. of data in Table 8.2). These numbers of data dropped to 9,223 and 1,292 respectively when only stations higher than 200 m are considered (Table 8.3).

**Table 8.2** Regression coefficients and explained variance  $R^2$  for the five separate regions and combined regions

All stations						
	No. of data	A1	A2	B	$R^2$	Significance of model
W1	5,319	0.014 (0.000)	0.834 (0.000)	-5.896 (0.000)	0.491	0.000
W2	7,231	0.001 (0.153)	1.049 (0.000)	-4.063 (0.000)	0.563	0.000
W3	7,866	0.001 (0.886)	1.100 (0.000)	-9.089 (0.000)	0.573	0.000
W123	20,416	0.005 (0.000)	0.973 (0.000)	-6.273 (0.000)	0.543	0.000
E1	2,127	0.001 (0.950)	1.120 (0.000)	-30.174 (0.000)	0.597	0.000
E2	1,377	0.014 (0.000)	1.050 (0.000)	-18.949 (0.000)	0.627	0.000
E12	3,504	0.004 (0.086)	1.080 (0.000)	-22.912 (0.000)	0.604	0.000

The numbers in parentheses are the statistical significances for individual coefficients, and the number of data input to each regression analysis is also shown

**Table 8.3** As in Table 8.2 except for rain stations with altitudes higher than 200 m

Stations >200 m						
	No. of data	A1	A2	B	$R^2$	Significance of model
W1	2,443	0.033 (0.000)	0.695 (0.000)	-15.142 (0.000)	0.440	0.000
W2	4,084	0.011 (0.000)	0.918 (0.000)	-10.961 (0.000)	0.514	0.000
W3	2,696	0.002 (0.346)	1.110 (0.000)	-13.867 (0.000)	0.569	0.000
W123	9,223	0.016 (0.000)	0.877 (0.000)	-15.622 (0.000)	0.511	0.000
E1	597	0.018 (0.011)	1.087 (0.000)	-60.946 (0.000)	0.615	
E2	695	0.020 (0.000)	1.030 (0.000)	-29.086 (0.000)	0.642	
E12	1,292	0.015 (0.000)	1.039 (0.000)	-36.028 (0.000)	0.624	

Comparison between Tables 8.1 and 8.2 indicates that after adding the orographic term to climatology, the explained variance ( $R^2$ ) increases slightly when all rain stations are considered. However, when only the stations above 200 m are considered (Table 8.3), the increase in explained variances are more than

marginal, and this applies to almost all sub-regions. Note that when interpreting the regression coefficients, their magnitudes do not reflect the relative importance of the variables. For example, the coefficients for orographic term are always much lower than those for climatology because the rain estimates from the orographic flux formula are much higher than reasonable rainfall amount (Cheung and McAneney 2008), and thus the coefficients serve to scale down to near-climatology values.

A noteworthy point is that the coefficients for region W3 (southwestern Taiwan) and to certain degree W2 (western Taiwan) are always very small compared with other regions. That is, the contribution from topographic effect is minimal in these two regions as shown by our regression analyses. However, extreme rainfall events associated with TCs did occur in southwestern Taiwan [e.g., Typhoon Mindulle (2004) that is discussed in Cheung et al. (2008) and the recent Typhoon Morakot (2009)] and as a matter of fact that region is the most disastrous area that suffers from heavy rainfall. It is believed that other mechanisms other than topographic effect are enhancing the rainfall in that region.

The above conclusion in regard to the southwestern regions in Taiwan is also confirmed by statistical significance tests for the regression models. The values of statistical significance given in Tables 8.2 and 8.3 represent the probability that the predicted values from the regression model or the individual regression coefficients are from a random distribution. It can be seen from Tables 8.2 and 8.3 that no matter when all stations or only those with high altitudes are considered, the regression models are statistical significant for all regions. This certainly makes sense since it is known that at least the rainfall climatology in the regression model accounts for a large portion of rainfall variance. However, the confidence level associated with the coefficient A1 for region W3 (and for E1 and W2 in the all-station model), which scales the contribution from orographic rain, is quite low. This recapitulates the early point that for southwestern Taiwan, adding the orographic lifting term to the regression model does not help much because they are not very different from adding a random variate. One effect not considered in this model comes from the summer southwesterly monsoon that coincides much with the peak typhoon season such that this kind of effects is most easily manifested. For region E1 (northeastern Taiwan), the non-effectiveness of adding the orographic term in the regression model may be due to effects from the winter northeasterly monsoon, which have been discussed in Cheung et al. (2008) and Wu et al. (2009). However, there are always fewer typhoon occurrences in the winter season and thus the number of late-season typhoons with rainfall distribution deviated much from climatology and simple orographic estimation is relatively small. Nevertheless, the statistical significance of the orographic term in the high-altitude regression model is valid at confidence level of nearly 99 %, which indicates that consideration of topographic effect in this region is still critical.

Besides a quantitative understanding of the relative contribution from climatology and topographic effect to TC rainfall, the established multiple regression models can be applied as an improved forecast tool to R-CLIPER. In particular, since regionally specific models are available, improvements in terms of the more

localized topographic effects can be expected when the W1–W3 and E1–E2 models are combined into one for the entire Taiwan area. These have been illustrated in Chang et al. (2011) with several TC cases.

### ***8.4.3 Importance of Remote-Sensing Techniques and Data***

The development of the Taiwan R-CLIPER and the subsequent multiple regression analyses benefit from the high-resolution network of automatic rain station. However, for regions with less density of rain stations such as in China, the ability of station-based rainfall climatology to resolve the rainfall distributions from TCs will be much reduced. Therefore, a major effort in research recently is to develop satellite-based algorithms for rain rate estimation that take into account the effects of land. Two recent studies are briefly summarized here. Jiang et al. (2008) investigated whether the ‘rainfall potential’ derived from the NASA TRMM multisatellite precipitation analysis is capable of predicting TC rainfall overland. The ‘rainfall potential’ is defined by using the satellite-derived rain rate, the satellite-derived storm size, and the storm translation speed. A total of 37 TCs that impacted the U.S. were examined and rainfall distributions for overland and over ocean are compared. It is found that the TC rainfall over ocean has a stronger relationship with TC intensity. Nevertheless, high correlations between rain potentials before landfall, in particular on the day prior to landfall, and the maximum storm total rain overland are identified. A TC overland rainfall index is introduced based on the satellite-derived rain potential. This technique will be useful when R-CLIPER-type model is extended to other regions without access to in situ rain gauge observations needed to develop the rainfall climatology or the rain gauge density is small.

Yu et al. (2009) compared the precipitation retrievals from three satellite datasets: the TRMM algorithm 3B42, the Climate Prediction Center Morphed (CMORPH) product, and a methodology based on the Geostationary Meteorological Satellite-5 infrared brightness temperature data (GMS5-TBB) developed by the Shanghai Typhoon Institute. The verification of the three datasets was based on rain gauge measurement associated with 50 TCs that affected China during 2003–2006, with 25 of them actually made landfall. It is found that in general the three datasets are able to provide reasonable rainfall distribution over land, but the skill of rain estimate decreases with latitude and rainfall amount. Because the TRMM-3B42 algorithm applies rain gauge adjustment, it has slightly better skill than the CMORPH dataset. However, both the TRMM-3B42 and CMORPH underestimate moderate to heavy rainfall but overestimate light precipitation. The GMS5-TBB method first analyzes the spatial structure of infrared brightness temperature data to identify the convective core and associated rain rate. For non-convective area, stratiform rain rate is also estimated. For rainfall over land associated with landfalling TCs, the method also adjusts the satellite estimates by rain gauge data. The result is that the GMS5-TBB method overestimates light

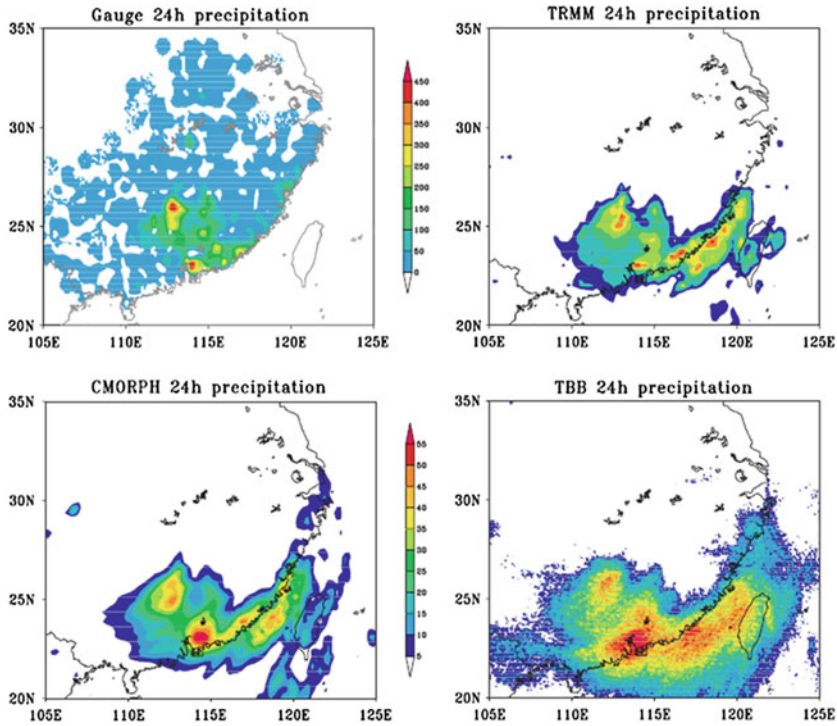


**Fig. 8.10** Comparison of the 24-h accumulated rainfall associated with Typhoon Bilis during 14–15 Jul 2006 from the four datasets of rain gauge, TRMM-3B42, CMORPH, and GMS5-TBB, respectively [adapted from Yu et al. (2009)]

precipitation more than the TRMM-3B42 and CMORPH, but performs much better than the other two algorithms in estimating heavy rainfall events. An example of Typhoon Bilis (2006) was given in Yu et al. (Fig. 8.10), which showed that the maximum accumulated rainfall estimate of 200–300 mm from GMS5-TBB at South China is much closer to the rain gauge measurement of about 400 mm than the other two methods.

## 8.5 Impacts from Global Changes

The future impacts from TCs under global changes depend on a lot of factors that include changes in the characteristics of TC activity, vulnerability of the coastal areas and resilience of our community to TC-related hazards. In recent years there have been debates on whether anthropogenic global warming (AGW) is modifying global TC activities, and in which aspects such as frequency and intensity are mostly affected (e.g., Emanuel 2005; Webster et al. 2005; Landsea 2005; Chan

2006; Vecchi et al. 2008; Knutson et al. 2010). The major argument against AGW influence to TC activity is that the latter is changing according to the natural decadal variability of the climate system, and hence heightened TC activity in a decade does not imply monotonic increase in TC frequency or intensity. In order to understand how AGW influences future TC activity but with reliable TC data only in recent decades, using climate models for simulating decadal change in TC activity under normal and warming climate becomes a popular technique in recent years. Since 2006, there have been studies from international research groups that utilized either atmospheric general circulation models with observed or projected sea surface temperature (Oouchi et al. 2006; Bengtsson et al. 2007a, b; LaRow et al. 2008; Zhao et al. 2009; Murakami and Wang 2010), ocean–atmosphere coupled models (e.g., Gualdi et al. 2008), and those that used regional downscaling (Emanuel et al. 2008; Bender et al. 2010). For warm-climate simulations, these studies basically agree on a reducing trend of global TC frequency (e.g., Knutson et al. 2008) but deviations exist on regional trends as well as the frequency of the intense cyclones. Diagnoses of these model simulations indicate that the overall reduction in TC frequency is related to increase in the convective inhibition of the atmosphere (Gualdi et al. 2008). Besides TC intensity, studies on the long-term trends in rainfall associated with TCs under climate change scenarios are also carried out (Hasegawa and Emori 2005; Gualdi et al. 2008). The recent summary by the expert team established by the World Meteorological Organization states that the higher-resolution modeling studies typically project substantial increases in the frequency of the most intense cyclones, and increases of the order of 20 % in the precipitation rate within 100 km of the storm center (Knutson et al. 2010). That is, more extreme convection episodes will occur in future TCs. Given this likely increase in TC rainfall under global changes, what are the roles played by the statistical rainfall models? Although these statistical models, such as those discussed herein, generally are not able to reproduce all of the extreme rainfall in TCs, they are capable for applications in estimating future TC-related rainfall scenarios. For example, it is convenient in execution of the statistical models such that a large number of simulations can be carried out for estimating future rainfall footprints in a particular region if there are changes in the TC tracks as identified in Murakami and Wang (2010). When more sophisticated statistical rainfall models that consider environment influences such as vertical wind shear, topography and synoptic effects like monsoonal flows, the models will continue to serve the forecast community for real-time mitigation, risk analysis as well as analyzing impacts of global change.

## 8.6 Summary

The torrential rainfall associated with landfalling TCs often represents the major impact to coastal regions, but at the same time an enormous challenge to meteorologists and forecasts. This chapter first describes the dissipation process of TCs

over land, and then discusses the complex dynamical processes involved in TC landfalls. These dynamical processes are introduced by the increased surface roughness and reduced surface moisture fluxes of land. Whereas each of these effects has quite straightforward impacts to the TC dynamical and convective structure, when they combine the resultant behavior of the TC is much less predictable. On one hand the effects from the land-sea contrast are interacting with the cyclonic circulation of the TC, on the other hand continuous feedback processes between the TC circulation and the ambient environment add substantial complexity to the problem. Although there have been a large number of observational and numerical studies on TC landfall in the last few decades, there is no single theory or conceptual model that can explain the asymmetry in convection and rainfall distribution of landfalling TCs in all ocean basins well.

The development of rainfall prediction techniques according to the needs of mitigation is emphasized in this chapter. Thus, after reviewing the requirements on the skill of rainfall forecasts from the perspectives of mitigation, the operation and performance of several statistical TC rainfall models are discussed. These include the PHRaM for predicting Atlantic hurricane rainfall, the R-CLIPER for the Taiwan area and the effort to introduce a component in R-CLIPER to consider topographic effect. While the R-CLIPER can usually explain 50–60 % of rainfall variance, the additional topographic component improves the model's performance in reproducing the local extreme rain that is lacking in the original model. Whereas NWP models are improving rapidly in terms of rainfall prediction, this kind of statistical models such as PHRaM and R-CLIPER has the advantage of efficiency in generating a large number of different rainfall scenarios such that they are not only applicable in real-time mitigation, but for risk analyses under the consideration of global changes as well.

**Acknowledgments** The first two authors (KKWC and LTCC) would like to thank Swiss Re for supporting their work on the rainfall climatology-persistence model. The continuous encouragement, support and comments from Prof. John McAnaney of the Risk Frontiers Natural Hazards Research Centre of Macquarie University are much appreciated. The third author (YL) is supported by the Higher Degree Research project support fund of Macquarie University. The third author (YL) was supported by a Macquarie University Research Excellence Scholarship (MQRES) and Higher Degree project support fund. YL is currently supported by a postdoctoral fellowship from the City University of Hong Kong.

## References

- Bender, M.A., Tuleya, R.E., Kurihara, Y.: A numerical study of the effect of a mountain range on a landfalling tropical cyclone. *Mon. Wea. Rev.* **113**, 567–583 (1985)
- Bender, M.A., Tuleya, R.E., Kurihara, Y.: A numerical study of the effect of island terrain on tropical cyclones. *Mon. Wea. Rev.* **115**, 130–155 (1987)
- Bender, M.A., Knutson, T.R., Tuleya, R.E., Sirutis, J.J., Vecchi, G.A., Garner, S.T., Held, I.M.: Modeled impact of anthropogenic warming on the frequency of intense atlantic hurricanes. *Science* **327**, 454–458 (2010)

- Bengtsson, L., Hodges, K.I., Esch, M.: Tropical cyclones in a T159 resolution global climate model: comparison with observations and reanalyses. *Tellus* **59A**, 396–416 (2007a)
- Bengtsson, L., Hodges, K.I., Esch, M., Keenlyside, N., Kornbluh, L., Luo, J.-J., Yamagata, T.: How many tropical cyclones change in a warmer climate? *Tellus* **59A**, 539–561 (2007b)
- Blackwell, K.G.: The evolution of Hurricane Danny (1997) at landfall: Doppler-observed eyewall replacement, vortex contraction/intensification, and low-level wind maxima. *Mon. Wea. Rev.* **128**, 4002–4016 (2000)
- Chan, J.C.L.: Comment on changes in tropical cyclone number, duration and intensity in a warming environment. *Nature* **311**, 1713 (2006)
- Chan, J.C.L.: Changes in track and structure of tropical cyclones near landfall. In: *Extended Abstract, 29th Conference on Hurricanes and Tropical Meteorology, Tuscon, Arizona, U.S., American Meteorological Society* (2010)
- Chan, J.C.L., Liang, X.: Convective asymmetries associated with tropical cyclone landfall. Part I: f-plane simulations. *J. Atmos. Sci.* **60**, 1560–1567 (2003)
- Chan, J.C.L., Liu, K.S., Ching, S.E., Lai, E.S.T.: Asymmetric distribution of convection associated with tropical cyclones making landfall along the south China coast. *Mon. Wea. Rev.* **132**, 2410–2420 (2004)
- Chang, C.P., Yeh, T.-C., Chen, J.-M.: Effects of terrain on the surface structure of typhoons over Taiwan. *Mon. Wea. Rev.* **121**, 734–752 (1993)
- Chang, L.T.-C., Chen, G.T.-J., Cheung, K.K.W.: Mesoscale simulation and moisture budget analyses of a heavy rain event over southern Taiwan in the Meiyu season. *Meteor. Atmos. Phys.* **101**, 43–63 (2008)
- Chang, L.T.-C., Cheung, K.K.W., McAneney, J.: A statistical analysis of the topographic effect on rainfall enhancement for tropical cyclones in the Taiwan area, p. 26, *Research Report for Swiss Re, Risk Frontiers Natural Hazard Research Centre, Macquarie University* (2011)
- Chang, S.: The orographic effects induced by an island mountain range on propagating tropical cyclones. *Mon. Wea. Rev.* **110**, 1255–1270 (1982)
- Chen, C.-Y., Lin, L.-Y., Yu, F.-C., Lee, C.-S., Tseng, C.-C., Wang, A.-X., Cheung, K.K.W.: Improving debris flow monitoring in Taiwan by using high-resolution rainfall products from QPESUMS. *Nat. Hazards* **40**, 447–461 (2007). doi:[10.1007/s11069-006-9004-2](https://doi.org/10.1007/s11069-006-9004-2)
- Chen, C.-Y., Chen, L.-K., Yu, F.-C., Lin, S.-C., Lin, Y.-C., Lee, C.-L., Wang, Y.-T., Cheung, K.W.: Characteristics analysis for the flash flood-induced debris flow. *Nat. Hazards* **47**, 245–261 (2008). doi:[10.1007/s11069-008-9217-7](https://doi.org/10.1007/s11069-008-9217-7)
- Cheung, K.K.W., McAneney, J.: Development of a statistical model for tropical cyclone rainfall in Taiwan for reinsurance loss analyses: preliminary results, p. 29, *Research Report for Swiss Re, Risk Frontiers Natural Hazard Research Centre, Macquarie University* (2008)
- Cheung, K.K.W., Huang, L.-R., Lee, C.-S.: Characteristics of rainfall during tropical cyclone periods in Taiwan. *Nat. Hazards Earth Syst. Sci.* **8**, 1463–1474 (2008)
- Dastoor, A., Krisnamurti, T.N.: The landfall and structure of a tropical cyclone: the sensitivity of model predictions to soil moisture parameterizations. *Boundary-Layer Meteorol.* **55**, 345–380 (1991)
- Dunn, G.E., Miller, B.I.: *Atlantic Hurricanes*, p. 377. Louisiana State University Press, Louisiana (1960)
- Ebert, E.E., Janowiak, J.E., Kidd, C.: Comparison of near-real-time precipitation estimates from satellite observations and numerical models. *Bull. Amer. Meteor. Soc.* **88**, 47–64 (2007)
- Emanuel, K.: Increasing destructiveness of tropical cyclones over the past 30 years. *Science* **436**, 686–688 (2005)
- Emanuel, K., Sundararajan, R., Williams, J.: Hurricanes and global warming: results from downscaling IPCC AR4 simulations. *Bull. Amer. Meteor. Soc.* **89**, 347–367 (2008)
- Farfan, L.M., Zehnder, J.A.: An analysis of the landfall of Hurricane Nora (1997). *Mon. Wea. Rev.* **129**, 2073–2088 (2001)
- Gao, S., Meng, Z., Zhang, F., Bosart, L.F.: Observational analysis of heavy rainfall mechanisms associated with severe tropical storm Bilis (2006) after its landfall. *Mon. Wea. Rev.* **137**, 1881–1897 (2009)



- Gualdi, S., Scoccimarro, E., Navarra, A.: Changes in tropical cyclone activity due to global warming: results from a high-resolution coupled general circulation model. *J. Climate* **21**, 5204–5228 (2008)
- Hasegawa, A., Emori, S.: Tropical cyclones and associated precipitation over the western North Pacific: T106 atmospheric GCM simulation for present-day and doubled CO<sub>2</sub> climates. *SOLA* **1**, 145–148 (2005)
- Ho, F.P., Su, J.C., Hanevich, K.L., Smith, R.J., Richards, F.P.: Hurricane climatology for the Atlantic and Gulf Coasts of the United States, p. 195, NOAA Technical Report NWS 38 (1987)
- Jiang, H., Halverson, J.B., Simpson, J., Zipser, E.J.: Hurricane “rainfall potential” derived from satellite observations aids overland rainfall prediction. *J. Appl. Meteor. Climatol.* **47**, 944–959 (2008)
- Jones, R.W.: A simulation of hurricane landfall with a numerical model featuring latent heating by the resolvable scales. *Mon. Wea. Rev.* **115**, 2279–2297 (1987)
- Kaplan, J., DeMaria, M.: A simple empirical model for predicting the decay of tropical cyclone winds after landfall. *J. Appl. Meteor.* **34**, 2499–2512 (1995)
- Kaplan, J., DeMaria, M., Knaff, J.A.: A revised tropical cyclone rapid intensification index for the Atlantic and east Pacific basins. *Weather Forecast.* **25**, 220–241 (2010)
- Knutson, T., Sirutis, J., Garner, S., Weccchi, G., Held, I.: Simulated reduction in Atlantic hurricane frequency under twenty-first-century warming condition. *Nat. Geosci.* p. 22. (2008). doi:[10.1038/ngeo202](https://doi.org/10.1038/ngeo202)
- Knutson, T.R., McBride, J.L., Chan, J., Emanuel, K., Holland, G., Landsea, C., Held, I., Kossin, J.P., Srivastava, A.K., Sugi, M.: Tropical cyclones and climate change. *Nature Geosci.*, **3**. doi:[10.1038/ngeo779](https://doi.org/10.1038/ngeo779) (2010)
- Koteswaram, P., Gaspar, S.: The surface structure of tropical cyclones in the Indian area. *Ind. J. Meteor. Geophys.* **7**, 339–352 (1956)
- Krajewski, W.F., Gabriele, V., Smith, J.A.: RADAR-rainfall uncertainties. *Bull. Amer. Meteor. Soc.* **91**, 87–94 (2010). doi:[10.1175/2009BAMS2747.1](https://doi.org/10.1175/2009BAMS2747.1)
- Landsea, C.W.: Hurricanes and global warming. *Science* **438**, E11–E12 (2005)
- LaRow, T., Lim, Y.-K., Shin, D., Chassignet, E., Cocke, S.: Atlantic basin seasonal hurricane simulations. *J. Climate* **21**, 3191–3206 (2008)
- Lee, C.-S., Huang, L.-R., Shen, H.-S., Wang, S.-T.: A climatological model for forecasting typhoon rainfall in Taiwan. *Nat. Hazards* **37**, 87–105 (2006)
- Lee, C.-S., et al.: Improvements to a river basin and catchment-based quantitative precipitation forecast technique during meiyu and typhoon periods (I), p. 248, Research report for the Water Resources Agency, Taiwan, National Taiwan University (2008) (In Chinese, English abstract available)
- Li, Y., Cheung, K.K.W., Chan, J.C.L.: An observational study on tropical cyclone landfall processes in the northwestern Australian region. Presentation at the AMOS and MetSoc NZ Joint Conference: Extreme Weather, Te Papa, Wellington, New Zealand, Australian Meteorological and Oceanographic Society and the Meteorological Society of New Zealand (2011)
- Li, Y., Cheung, K.K.W., Chan, J.C.L., Tokuno, M.: Rainfall distribution of five landfalling tropical cyclones in the northwestern Australian region. *Aust. Met. Oceanog. J.* **63**, 325–338 (2013)
- Lin, Y.-L., Han, J.G., Hamilton, D.W., Huang, C.-Y.: Orographic influence on a drifting cyclone. *J. Atmos. Sci.* **56**, 534–562 (1999)
- Lin, Y.-L., Ensley, D.B., Chiao, S., Huang, C.-Y.: Orographic influences on rainfall and track deflection associated with the passage of a tropical cyclone. *Mon. Wea. Rev.* **130**, 2929–2950 (2002)
- Lonfat, M., Marks Jr, F.D., Chen, S.: Precipitation distribution in tropical cyclones using the Tropical Rainfall Measuring Mission (TRMM) microwave imager: a global perspective. *Mon. Wea. Rev.* **132**, 1645–1660 (2004)

- Lonfat, M., Rogers, R., Marchok, T., Marks Jr, F.D.: A parametric model for predicting hurricane rainfall. *Mon. Wea. Rev.* **135**, 3086–3097 (2007)
- Marchok, T., Rogers, R., Tuleya, R.: Validation schemes for tropical cyclone quantitative precipitation forecasts: evaluation of operational models for U.S. landfalling cases. *Weather Forecast.* **22**, 726–746 (2007)
- Marks Jr, F.D.: Evolution of the structure of precipitation in Hurricane Allen (1980). *Mon. Wea. Rev.* **113**, 909–930 (1985)
- Marks, F.D., Kappler, G., DeMaria, M.: Development of a tropical cyclone rainfall climatology and persistence (R-CLIPER) model. In: Preprints, 25th Conference Hurricane and Tropical Meteorology, pp. 327–328, San Diego, American Meteorological Society (2002)
- Miller, B.L.: A study of the filling of Hurricane Donna (1960) over land. *Mon. Wea. Rev.* **92**, 389–406 (1964)
- Murakami, H., Wang, B.: Future change of north Atlantic tropical cyclone tracks: projection by a 20 km-mesh global atmospheric model. *J. Climate* **23**, 2699–2721 (2010)
- Oouchi, K., Yoshimura, J., Yoshimura, H., Mizuta, R., Kusunoki, S., Noda, A.: Tropical cyclone climatology in a global-warming climate as simulated in a 20 km-mesh global atmospheric model: Frequency and wind intensity analyses. *J. Meteor. Soc. Japan* **84**, 259–276 (2006)
- Parrish, J.R., Burpee, R.W., Marks Jr, F.D., Grebe, R.: Rain patterns observed by digitized radar during the landfall of Hurricane Frederic (1979). *Mon. Wea. Rev.* **110**, 1933–1944 (1982)
- Powell, M.D.: The transition of the Hurricane Frederic boundary-layer wind field from the open Gulf of Mexico to landfall. *Mon. Wea. Rev.* **110**, 1912–1932 (1982)
- Powell, M.D.: Changes in the low-level kinematic and thermodynamic structure of Hurricane Alicia (1983) at landfall. *Mon. Wea. Rev.* **115**, 75–99 (1987)
- Ramsay, H.A., Leslie, L.M.: The effects of complex terrain on severe landfalling tropical cyclone Larry (2006) over Northeast Australia. *Mon. Wea. Rev.* **136**, 4334–4354 (2008)
- Rappaport, E.N., Franklin, J.L., Schumacher, A.B., DeMaria, M., Shay, L.K., Gibney, E.J.: Tropical cyclone intensity change before U.S. Gulf coast landfall. *Weather Forecast.* **25**, 1380–1396 (2010)
- Saffir, H.S.: Design and construction requirements for hurricane resistant construction, p. 20. American Society of Civil Engineers, Preprint Number 2830 (1977)
- Schwerdt, R.W., Ho, F.P., Watkinds, R.R.: Meteorological criteria for standard project hurricane and probable maximum hurricane windfields, Gulf and East Coasts of the United States, p. 317, NOAA Technical Report NWS 23 (1979)
- Simpson, R.H.: A proposed scale for ranking hurricanes by intensity. In: Minutes of the 8th NOAA, NWS Hurricane Conference, Miami, Florida, National Oceanic and Atmospheric Administration (1971)
- Tuleya, R.E., Kurihara, Y.: A numerical simulation of the landfall of tropical cyclones. *J. Atmos. Sci.* **35**, 242–257 (1978)
- Tuleya, R.E., DeMaria, M., Kuligowski, R.J.: Evaluation of GFDL and simple statistical model rainfall forecasts for US landfalling tropical storms. *Weather Forecast.* **22**, 56–70 (2007)
- Vecchi, G.A., Swanson, K.L., Soden, B.L.: Whither hurricane activity? *Science* **322**, 687–689 (2008)
- Wang, Y., Wu, C.-C.: Current understanding of tropical cyclone structure and intensity changes: a review. *Meteorol. Atmos. Phys.* **87**, 257–278 (2004)
- Webster, P.J., Holland, G.J., Curry, J.A., Chang, H.-R.: Changes in tropical cyclone number, duration and intensity in a warming environment. *Nature* **309**, 1844–1846 (2005)
- Wong, M.L.M., Chan, J.C.L., Zhou, W.: A simple empirical model for estimating the intensity change of tropical cyclones after landfall along the South China coast. *J. Appl. Meteor. Climatol.* **47**, 326–338 (2008)
- Wu, C.-C., Kuo, Y.-H.: Typhoons affecting Taiwan: current understanding and future challenges. *Bull. Amer. Meteor. Soc.* **80**, 67–80 (1999)
- Wu, C.-C.: Numerical simulation of Typhoon Gladys (1994) and its interaction with Taiwan terrain using the GFDL hurricane model. *Mon. Wea. Rev.* **129**, 1533–1549 (2001)

- Wu, C.-C., Yen, T.-H., Kuo, Y.-H., Wang, W.: Rainfall simulation associated with Typhoon Herb (1996) near Taiwan. Part I: the topographic effect. *Weather Forecast.* **17**, 1001–1015 (2002)
- Wu, C.-C., Cheung, K.K.W., Lo, Y.-Y.: Numerical study of the heavy rainfall event due to the interaction of Typhoon Babs (1998) and the northeasterly monsoon. *Mon. Wea. Rev.* **137**, 2049–2064 (2009)
- Yeh, T.-C., Elsberry, R.L.: Interaction of typhoons with the Taiwan orography. Part I: upstream track deflections. *Mon. Wea. Rev.* **121**, 3193–3212 (1993a)
- Yeh, T.-C., Elsberry, R.L.: Interaction of typhoons with the Taiwan orography. Part II: continuous and discontinuous tracks across the island. *Mon. Wea. Rev.* **121**, 3213–3233 (1993b)
- Yu, Z., Yu, H., Chen, P., Qian, C., Yue, C.: Verification of tropical cyclone-related satellite precipitation estimates in mainland China. *J. Appl. Meteor. Climatol.* **48**, 2227–2241 (2009)
- Zehnder, J.A.: The influence of large-scale topography on barotropic vortex motion. *J. Atmos. Sci.* **50**, 2519–2532 (1993)
- Zhao, M., Held, I.M., Lin, S.-J., Vecchi, G.A.: Simulations of global hurricane climatology, interannual variability, and response to global warming using a 50 km resolution GCM. *J. Climate* **22**, 6653–6678 (2009)